Osteoporosis and Sarcopenia 7 (2021) 121–126

Contents lists available at ScienceDirect

Osteoporosis and Sarcopenia

journal homepage: http://www.elsevier.com/locate/afos

Original article

Analysis of bone in adenine-induced chronic kidney disease model rats

Hikaru Saito , Naohisa Miyakoshi *, Yuji Kasukawa , Koji Nozaka , Hiroyuki Tsuchie , Chiaki Sato , Kazunobu Abe , Ryo Shoji , Yoichi Shimada

Department of Orthopedic Surgery, Akita University Graduate School of Medicine, 1-1-1, Hondo, Akita, 010-8543, Japan

ARTICLE INFO

Article history:
Received 16 August 2021
Received in revised form
13 October 2021
Accepted 3 November 2021
Available online 20 November 2021

Keywords:
Chronic kidney disease
Osteoporosis
Bone mineral density
Bone strength
Bone microstructure

ABSTRACT

Objectives: The purpose of this study is to investigate the stage of chronic kidney disease (CKD) in adenine-induced CKD model rats by serum analyses, and to examine bone mineral density (BMD), bone strength, and microstructure of trabecular and cortical bone in these rats.
Methods: Eight-week-old, male Wistar rats (n = 42) were divided into 2 groups: those fed a 0.75% adenine diet for 4 weeks until 12 weeks of age to generate CKD model rats (CKD group); and sham rats. The CKD and sham groups were sacrificed at 12, 16, and 20 weeks of age (n = 7 in each group and at 12, 16, and 20 weeks), and various parameters were evaluated, including body weight, renal wet weight, muscle wet weight, renal histology, biochemical tests, BMD, biomechanical testing, and micro-computed tomography (CT). The parameters were compared between the 2 groups at the various time points.
Results: In the CKD model rats, at 20 weeks of age, serum creatinine, phosphorus, and intact-PTH levels were elevated, and serum calcium levels were normal, indicating that the CKD was stage IV and associated with secondary hyperparathyroidism. Decreased BMDs of the whole body and the femur were observed as bone changes, and micro-CT analysis showed deterioration of bone microstructure of the cortical bone that resulted in decreased bone strength in the cortical and trabecular bone.
Conclusions: These CKD model rats showed stage IV CKD and appear appropriate for evaluating the effects of several treatments for CKD-related osteoporosis and mineral bone disorder.
© 2021 The Korean Society of Osteoporosis. Publishing services by Elsevier B.V. This is an open access article under the CC BY-NC-ND license (http://creativecommons.org/licenses/by-nc-nd/4.0/).

1. Introduction

Chronic kidney disease (CKD) is a worldwide health problem, especially in aged societies, and its incidence and prevalence have been increasing in elderly people [1]. In addition to the renal dysfunction of CKD, it is associated with the development of mineral bone disorder (MBD), osteoporosis, and an increased risk of fragility fractures [2,3]. It has been reported that the increased risk of fragility fractures in CKD patients is caused by not only bone loss [4,5], but also deterioration of bone quality, such as changes in the microstructure of bone, cortical porosity, mineralization, and collagen cross-linking [6–8]. The risk of fractures in CKD patients has been considered to be 2 to 14 times higher than that in the general population [3,9]. In particular, the incidence of fractures increases as the disease progresses to stage IV or higher, compared to CKD stage III or lower [10,11]. Therefore, it is very important to prevent the increased risk of fragility fractures, especially in CKD patients of stage IV or higher.

To prevent fragility fractures in CKD patients of stage IV or higher, it is necessary to elucidate the changes of bone mass and bone micro-structure in trabecular and cortical bone. However, it is impossible to investigate the details of trabecular and cortical bony changes in CKD patients. Therefore, rodent models of CKD are needed to investigate the changes of trabecular and cortical bone during CKD progression. Adenine-induced CKD model rats have advantages, such as the induction of CKD of varying severity and being able to maintain the stage for a certain period of time [12]. In this model, feeding a 0.75% adenine diet for 4 weeks induces non-progressive and irreversible renal failure. The kidneys in these adenine-induced CKD model rats were enlarged with interstitial inflammatory infiltrates and crystalline tubulointerstitial deposits [13], mimicking a mechanistic pathway of human CKD [14].

In regard to the severity stage of CKD, it has been considered that fibroblast growth factor 23 (FGF23) increases from CKD stage

* Corresponding author.
E-mail address: miyakosh@doc.med.akita-u.ac.jp (N. Miyakoshi).
Peer review under responsibility of The Korean Society of Osteoporosis.

https://doi.org/10.1016/j.afos.2021.11.001
2405-5255/© 2021 The Korean Society of Osteoporosis. Publishing services by Elsevier B.V. This is an open access article under the CC BY-NC-ND license (http://creativecommons.org/licenses/by-nc-nd/4.0/).

II, parathyroid hormone (PTH) levels rise from CKD stage III, hyperphosphatemia is observed in CKD stage IV, and hypocalcemia is obvious in CKD stage V [15,16]. However, in adenine-induced CKD model rats created by feeding an adenine diet for 4 weeks, it is still unclear whether stage IV CKD has occurred and how long the condition will continue, and to what extent the bone mineral density (BMD), bone microstructure, and bone strength of trabecular and cortical bone will deteriorate. Therefore, in this study, CKD model rats were created by feeding the rats an adenine diet for 4 weeks, and the stage of CKD and bone were analyzed. The purpose of this study is to investigate the stage of CKD in this model by serum analyses, and to examine BMD, bone strength, and microstructure of trabecular and cortical bone in these CKD model rats.

2. Methods

2.1. Animal model and experimental design

Eight-week-old, male Wistar rat (n = 42) (Charles River Laboratories Inc., Tokyo, Japan) were housed in a controlled environment (temperature 23 ± 2 °C, humidity 40% ± 20%) with a 12-h light-dark cycle with free access to water and rat food. The details were described in the previous study [17]. Rats were treated with a 0.75% adenine diet (Oriental Yeast Co., Ltd., Tokyo Japan) for 4 weeks until 12 weeks of age, followed by a standard rodent chow (CE-7; Clea Japan, Tokyo, Japan) regular diet to generate CKD model rats (CKD group). The 4-week treatment with the adenine diet was decided based on the previous study [12], which reported that the 4-week treatment with the adenine diet induced non-progressive, irreversible renal failure. The CKD and sham groups were sacrificed at 12, 16, and 20 weeks of age (n = 7 in each group and at 12, 16, and 20 weeks), and the following parameters were evaluated. The protocols for all animal experiments were approved in advance by the Animal Experimentation Committee at our institute (permit number a-1-3070), and all subsequent animal experiments adhered to the Guidelines for Animal Experimentation of our institute.

2.2. Body weight, renal wet weight, and muscle wet weight measurement

Body weight (BW) was measured at 12, 16, and 20 weeks of age. The difference in BW between the CKD and sham groups was evaluated, and the BW of each group at each week was compared. The right kidney was harvested, and its wet weight was measured after the ureter and blood vessels were removed. Tibialis anterior and soleus muscles were harvested at their tendon attachments, and their wet weights were measured at sacrifice each time.

2.3. Tissue preparation

After sacrifice, the right femur and lumbar vertebrae (L2-4) were fixed in 10% neutral-buffered formalin (Wako Chemical Industries, Osaka, Japan) until preparation for BMD and micro-computed tomography (CT) measurement. The left femur was dissected free of soft tissue, wrapped in gauze moistened with saline, and frozen at − 80 °C until biomechanical testing. The right kidney was weighed and then fixed in 10% neutral-buffered formalin to prepare renal tissue sections. The right tibialis anterior and soleus muscles were removed and weighed.

2.4. Renal histology

Three-micrometer-thick sections were stained with hematoxylin and eosin (H&E) and Elastica-Masson stains. To assess the degree of the tubulointerstitial disorder, the fibrotic area was expressed as fibrotic area/total area × 100 (%), as previously described [18] in an Elastica-Masson-stained section. A magnification of 40x was used for this measurement. An average of the 3 regions of interest (ROI) selected randomly in each section was used as a parameter for the percentage of renal fibrosis. Fibrotic areas were measured using a Keyence BZ-X800 microscope and BZ-X800 Analyzer software (Keyence Corp., Osaka, Japan).

2.5. Biochemical analysis

Blood samples were collected from the vena cavae of rats at 12, 16, and 20 weeks of age. The blood samples were centrifuged at 3,000 rpm for 30 min at 4 °C to separate the serum and then stored in single-use aliquots at −80 °C until analysis. Blood urea nitrogen (BUN), creatinine (CRE), calcium (Ca), and inorganic phosphorus (IP) levels were measured using a Hitachi Automatic Biochemical Analyzer 7180 (Hitachi Ltd., Tokyo, Japan). Intact-parathyroid hormone (I-PTH) levels were measured using an enzyme-linked immunosorbent assay (ELISA) kit (Rat Intact PTH ELISA Kit, Immutopics, Inc. San Clemente, CA, USA).

2.6. BMD measurement

Whole-body BMD was measured using dual-energy X-ray absorptiometry (QDR 4500 Delphi; Hologic, Bedford, MA, USA). Rats were scanned in “small animal” mode, with the “regional high resolution” scan option.

2.7. Biomechanical testing

The compression test of the distal part of the left femur was performed at room temperature using a material testing machine (MZ500S; Maruto, Tokyo, Japan) at 12, 16, and 20 weeks of age, as previously described [19–21]. Load-displacement curves were recorded, and the maximum load (N), stiffness (N/mm), and energy absorption (N.mm) were calculated using software for measuring bone strength (CTR win. Version 1.05; System Supply, Nagano, Japan).

2.8. Micro-computed tomography analysis

The excised right distal femurs from rats in the sham and CKD groups at 20 weeks of age were secured in a sample holder. Micro-CT was performed with CosmoScan GX II (Rigaku Corporation, Tokyo, Japan), according to the manufacturer's instructions, with an isotropic voxel size of 36 μm, energy of 90 kVp, and current of 88 μA, following the previous reports [20,22]. The captured images were rendered using TRI/3D BON software (Ratoc System Engineering Co., Ltd., Tokyo, Japan). Evaluation of osteoporosis was performed based on the volumetric BMD (vBMD) and total area (Tt.Ar), cortical area (Ct.Ar), cortical thickness (Ct.Th), and cortical porosity as parameters of cortical bone, and bone volume/tissue volume (BV/TV), trabecular thickness (Tb.Th), trabecular number (Tb.N), trabecular separation (Tb.Sp), structure model index (SMI), and connectivity density (Conn.D) as parameters of trabecular bone, at the distal femur.

2.9. Statistical analysis

All data are expressed as means ± standard deviation (SD). A Kolmogorov-Smirnov test showed that all data were normally distributed. Comparisons of data between the sham and CKD groups were performed using Student's *t*-test. Comparisons of data among the sham and CKD groups were performed using one-way

analysis of variance (ANOVA) and Tukey's post hoc test. All statistical analyses were performed with EZR [23], which is a modified version of R commander designed to add statistical functions frequently used in biostatistics. Values of $P < 0.05$ were considered significant.

3. Results

3.1. Body weight, renal wet weight, and skeletal muscle weight

Table 1 shows the results of body weight, renal wet weight, and skeletal muscle wet weight.

Although the body weights of sham and CKD rats were significantly increased during the experiment ($P = 0.002$ and $P < 0.001$, respectively), the body weights of CKD rats were significantly lower than of sham rats from 12 to 20 weeks ($P < 0.05$). Renal wet weight and renal wet weight per body weight were significantly higher in the CKD rats than in the sham rats ($P < 0.05$ and $P < 0.05$, respectively), and they decreased significantly in a time-dependent manner during the experiment ($P < 0.001$ and $P < 0.001$, respectively). The tibialis anterior and soleus muscle wet weights were significantly increased both in the sham and CKD rats during the experiment ($P = 0.007$ ~ $P < 0.001$), and these skeletal muscle wet weights were significantly lower in the CKD rats than in the sham rats ($P < 0.05$). When these skeletal muscle wet weights were adjusted by body weight, there were no significant differences between the sham and CKD rats, except for soleus muscle wet weight per body weight at 12 weeks, during the experiment.

3.2. Histological sections of kidney and percentage of renal fibrosis

Histological sections of kidneys in the sham rats at 20 weeks demonstrated normal findings on H&E-stained sections (Fig. 1A) and less fibrosis of renal stroma on Elastica-Masson-stained sections (Fig. 1B). On the other hand, there was enlargement of the urinary cavities on the H&E-stained sections (Fig. 1C) and fibrosis of the renal interstitium on the Elastica-Masson-stained sections (Fig. 1D) in CKD rats at 20 weeks.

The percentage of fibrosis of the renal interstitium was significantly higher in the CKD rats than in the sham rats ($P = 0.025$ to $P < 0.001$), and the percentage was significantly increased in the CKD rats in a time-dependent manner from 12 weeks to 20 weeks ($P < 0.01$) (Fig. 1E).

3.3. Serum markers

Results of serum markers are shown in Table 2. In the sham rats, only CRE was significantly increased during the experiment from 12 weeks to 20 weeks ($P = 0.015$), but the other parameters did not change significantly. However, in the CKD rats, BUN, CRE, IP, and I-PTH peaked at 12 weeks and decreased significantly at 16 and 20 weeks, except I-PTH, on ANOVA ($P < 0.001$). The Ca++ level was its lowest at 12 weeks and significantly higher at 16 and 20 weeks ($P < 0.001$) in the CKD rats. The BUN, CRE, IP (except at 16 weeks), and I-PTH levels were significantly higher in the CKD rats than in the sham rats from 12 to 20 weeks ($P < 0.05$).

3.4. BMD

Whole-body BMD increased significantly in the sham and CKD rats during the experiment from 12 weeks to 20 weeks by ANOVA ($P < 0.001$) (Table 3). Whole-body BMD was significantly lower in the CKD rats than in the sham rats at 12, 16, and 20 weeks ($P < 0.05$).

3.5. Microstructure of trabecular and cortical bone

Table 4 shows the results of micro-CT at the distal metaphysis of the femur at 20 weeks of age. The vBMD, Ct.Ar/Tr.Ar, Ct.Th, and Ct.Ar were significantly lower in the CKD rats than in the sham rats ($P < 0.05$). On the other hand, there were no significant differences in bone volume (BV/TV) and parameters of microarchitecture (Tb.Th, Tb.N, Tb.Sp, SMI, and Conn D) between CKD and sham rats; only vBMD at the distal metaphysis was significantly lower in the CKD rats than in the Sham rats ($P = 0.009$).

3.6. Bone strength

The results of the compression test of the distal metaphysis of the femur are shown in Table 5. All parameters of bone strength on the compression test, both in the sham and CKD rats, were significantly increased during the experiment from 12 weeks to 20 weeks on ANOVA ($P = 0.011$ to $P < 0.001$). Bone strength evaluated by the breaking energy and that measured by maximum load in the CKD rats were significantly impaired compared with those in the sham rats only at 12 and 20 weeks. Stiffness by the compression test was significantly lower in the CKD rats than in the sham rats only at 16 weeks ($P < 0.05$).

4. Discussion

4.1. Summary of the present study

In the present study, the stage of CKD and trabecular and cortical bone changes were evaluated in CKD model rats, established by feeding a 0.75% adenine diet for 4 weeks from 8 weeks of age to male Wistar rats, following previous reports [12]. On blood tests at 20 weeks of age, serum creatinine, phosphorus, and I-PTH levels were elevated, and serum calcium levels were normal, indicating

Table 1
Body weight, renal weight, and skeletal muscle weight.

	Sham (n = 7)			P-value	CKD (n = 7)			P-value
	12 W	16 W	20 W	ANOVA	12 W	16 W	20 W	ANOVA
Body weight, g	464.9 ± 8.7	538.9 ± 57.2[a]	576.0 ± 62.6[a]	0.002	200.5 ± 13.3*	431.6 ± 19.7[a]*	492.0 ± 29.1[a,b]*	< 0.001
Renal wet weight, g	1.6 ± 0.1	1.7 ± 0.2	1.8 ± 0.2	0.145	3.6 ± 0.6*	2.6 ± 0.3[a]*	2.2 ± 0.4[a]*	< 0.001
Renal wet weight/body weight, %	0.34 ± 0.03	0.30 ± 0.04	0.31 ± 0.02	0.090	1.82 ± 0.29*	0.60 ± 0.09[a]*	0.45 ± 0.09[a,b]*	< 0.001
Muscle wet weight								
Tibialis anterior, g	0.91 ± 0.07	1.04 ± 0.13	1.11 ± 0.08[a]	0.007	0.39 ± 0.03*	0.80 ± 0.07[a]*	0.97 ± 0.10[a,b]*	< 0.001
Soleus, g	0.21 ± 0.02	0.22 ± 0.03	0.28 ± 0.03[a,b]	< 0.001	0.12 ± 0.02*	0.19 ± 0.01[a]*	0.25 ± 0.02[a,b]*	< 0.001
Muscle wet weight/body weight								
Tibialis anterior, %	0.196 ± 0.012	0.194 ± 0.007	0.193 ± 0.018	0.937	0.194 ± 0.006	0.186 ± 0.009	0.197 ± 0.011	0.190
Soleus, %	0.045 ± 0.004	0.041 ± 0.003	0.049 ± 0.002[a,b]	< 0.001	0.061 ± 0.010*	0.044 ± 0.003[a]	0.050 ± 0.003[a,b]	< 0.001

Values are mean ± standard deviation.
a: $P < 0.05$ vs 12 W, b: $P < 0.05$ vs 16 W in the sham or CKD group by post hoc test.
*: $P < 0.05$ vs sham at the same weeks by unpaired *t*-test.

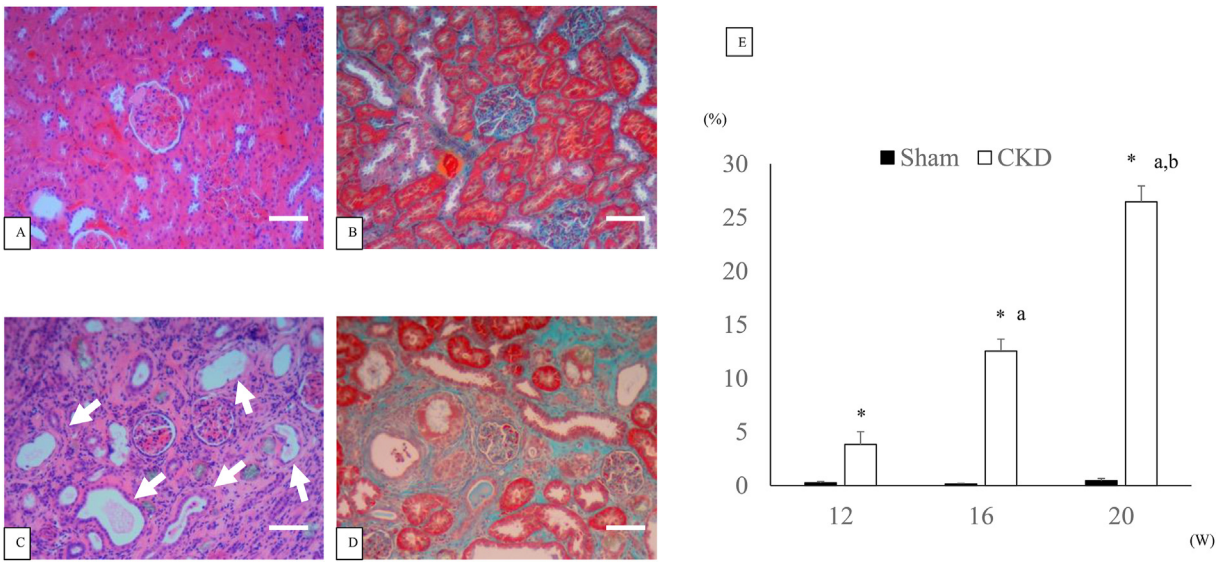

Fig. 1. Histological section of kidney and quantitative analysis of the fibrotic area in the kidney, Representative section stained with hematoxylin and eosin (H&E) or Elastica-Masson stain of the kidney in the sham and chronic kidney disease (CKD) rats. A: H&E-stained section of the sham rats. B: Elastica-Masson-stained section of the sham rats. C: H&E-stained section of the CKD rats. D: Elastica-Masson-stained section of the CKD rats. White arrows: tubular lumen. Scale bar is 100 μm. E: Percentage of fibrotic area in the kidney. Black bar: sham rats, White bar: CKD rats. a: P < 0.05 vs 12 W, b: P < 0.05 vs 16 W in the sham or CKD group by post hoc test. *: P < 0.05 vs sham at the same weeks by unpaired *t*-test.

Table 2
Serum biochemical markers.

	Sham (n = 7)			P-value	CKD (n = 7)			P-value
	12 W	16 W	20 W	ANOVA	12 W	16 W	20 W	ANOVA
BUN, mg/dL	19.8 ± 4.7	17.1 ± 1.6	17.9 ± 3.2	0.380	141.7 ± 28.5*	34.9 ± 8.8[a]*	37.9 ± 7.2[a]*	< 0.001
CRE, mg/dL	0.30 ± 0.03	0.35 ± 0.04[a]	0.35 ± 0.03[a]	0.015	2.19 ± 0.35*	0.80 ± 0.15[a]*	0.80 ± 0.18[a]*	< 0.001
Ca, mg/dL	11.1 ± 0.6	11.4 ± 0.8	10.8 ± 0.6	0.503	4.8 ± 0.5*	11.8 ± 0.4[a]	11.0 ± 0.4[a,b]	< 0.001
IP, mg/dL	8.4 ± 1.1	8.0 ± 1.1	7.0 ± 1.0	0.080	34.2 ± 6.0*	9.2 ± 1.4[a]	8.1 ± 0.6[a]*	< 0.001
I-PTH, pg/mL	419.2 ± 299.9	713.2 ± 423.4	463.4 ± 273.7	0.314	2325.4 ± 228.2*	1820.3 ± 655.3*	1634.9 ± 542.6*	0.058

Values are mean ± standard deviation.
a: P < 0.05 vs 12 W, b: P < 0.05 vs 16 W in the sham or CKD group by post hoc test.
*: P < 0.05 vs sham at the same weeks by unpaired *t*-test.
BUN: blood urea nitrogen, CRE: creatinine, Ca: calcium, IP: inorganic phosphorus, I-PTH: intact parathyroid hormone.

Table 3
Whole-body bone mineral density (BMD).

	Sham (n = 7)			P-value	CKD (n = 7)			P-value
	12 W	16 W	20 W	ANOVA	12 W	16 W	20 W	ANOVA
BMD, mg/cm^2	0.159 ± 0.005	0.170 ± 0.006[a]	0.184 ± 0.007[a,b]	< 0.001	0.136 ± 0.007*	0.156 ± 0.005[a]*	0.169 ± 0.004[a,b]*	< 0.001

Values are mean ± standard deviation.
a: P < 0.05 vs 12 W, b: P < 0.05 vs 16 W in the sham or CKD group by post hoc test.
*: P < 0.05 vs sham at the same weeks by unpaired *t*-test.

that the CKD was stage IV and associated with secondary hyperparathyroidism. Decreased BMDs of the whole body and the femur were observed as bone changes, and micro-CT analysis showed deterioration of bone microstructure of the cortical bone that resulted in decreased bone strength in the cortical and trabecular bone at the distal femur.

4.2. Adenine's effects on renal failure, serum parameters, and CKD stage

After 4 weeks of feeding with a 0.75% adenine diet, the kidneys were swollen, and the histological sections showed interstitial fibrosis and enlargement of tubular lumens in the renal tissue. These findings are the same as the already reported histological findings of the kidney in previous reports [13,14]. Serum BUN and CRE levels were high at 12 weeks of age, and they then gradually decreased at 16 weeks to 20 weeks of age, but they were still high at 20 weeks of age, indicating continued renal dysfunction. Based on these changes in serological findings, administration of the adenine diet for 4 weeks from 8 weeks of age appeared to have caused severe renal damage as a state of acute renal failure. Although some renal function recovered, it did not return to normal renal function as a stage of chronic renal failure at 20 weeks of age. I-PTH continued to be high from 12 to 20 weeks of age, and it is considered that the state of secondary hyperparathyroidism was maintained from 12 weeks to 20 weeks of age in these CKD model rats. These changes of serum markers indicate that the adenine-induced renal failure partially recovered and considered to be a mixed model of acute to chronic renal failure. Therefore, if bone tissues and serum markers are evaluated at further intervals in these

Table 4
Micro-computed tomography at the distal metaphysis of the femur.

	Sham (n = 7)	CKD (n = 6)	P-value vs Sham
Cortical bone			
vBMD, mg/cm^3	888.4 ± 23.8	838.4 ± 20.8	0.002
Tt.Ar, mm^2	6.2 ± 0.5	6.2 ± 0.3	0.778
Ct.Ar/Tt.Ar, %	39.6 ± 2.2	35.8 ± 1.2	0.003
Ct.Th, μm	297.5 ± 19.4	269.8 ± 14.9	0.016
Ct.Ar, mm^2	2.5 ± 0.1	2.2 ± 0.2	0.011
Cortical porosity, %	3.4 ± 4.0	3.6 ± 0.3	0.421
Trabecular bone			
vBMD, mg/cm^3	660.9 ± 11.8	630 ± 22.4	0.009
BV/TV, %	11.7 ± 4.7	9.8 ± 2.6	0.388
Tb.Th, μm	51.9 ± 1.5	50.6 ± 1.4	0.133
Tb.N, 1/mm	1.8 ± 0.5	1.9 ± 0.5	0.827
Tb.Sp, μm	134.4 ± 44.8	108.3 ± 13.9	0.200
SMI	2.2 ± 0.2	2.4 ± 0.1	0.120
Conn.D, 1/mm^3	97.6 ± 57.6	61.3 ± 31.0	0.196

Values are mean ± standard deviation.
vBMD, volumetric bone mineral density; Tt.Ar, total area; Ct.Ar/Tt.Ar, cortical area/total area; Ct.Th, cortical thickness; Ct.Ar, cortical area; BV/TV, bone volume/tissue volume; Tb.Th, trabecular thickness; Tb.N, trabecular number; Tb.Sp, trabecular separation; SMI, structure model index; Conn.D, connectivity density.

adenine-induced CKD model rats, there is a possibility that renal failure at a younger age can be a model for examining the effects on bone and mineral metabolism in later years.

4.3. Changes of trabecular BMD, bone strength, and micro-architecture

The increased risk of fractures in CKD patients cannot be evaluated by measuring BMD alone, and there is no consensus on the effects of CKD on trabecular BMD or trabecular bone-related parameters. In the 2-year clinical study of changes in cortical and trabecular bone mass in dialysis patients with CKD, although the BMDs were decreased 5.9% in the total femur and 10.0% in the cortical bone of the femur, the BMD of trabecular bone was increased 5.9% at the femur [24]. In CKD model animals, there is a report that the bone mass of trabecular bone did not change or rather increased in 5/6 nephrectomized rats [25,26]. In addition, Bajwa et al. [27] demonstrated that trabecular bone mass in the 5/6 nephrectomized rats fed a high phosphorus diet was decreased, but not in those fed a normal diet. In adenine-induced CKD model rats, Ni et al. [28] reported that the BMDs of femurs and lumbar vertebrae were significantly reduced, and the trabecular parameters including BV/TV, trabecular thickness, and trabecular number were decreased at 42 weeks after 4 weeks of feeding with 0.75% adenine and a high-phosphorus diet. Metzger et al. [29] reported that adenine-induced CKD model male rats showed lower trabecular BV/TV, lower trabecular thickness, higher trabecular separation, and lower trabecular number compared to control male rats. On the other hand, trabecular bone volume was higher in female B6 mice fed 0.2% adenine for 6 weeks than in B6 controls, whereas C3H mice fed with adenine had lower trabecular bone volume than C3H controls [30]. Ferrari et al. [31] compared the changes of trabecular bone between the 5/6 nephrectomized rats and adenine-induced CKD model rats. Their study showed that the adenine-induced CKD model rats had a higher bone formation rate and higher bone resorption area, as well as osteoclast area, than the 5/6 nephrectomized CKD model rats. Although there was no significant difference in the trabecular bone volume between the 2 groups, the adenine-induced CKD model rats had lower trabecular number and higher trabecular separation compared to the 5/6 nephrectomized rats. The study concluded that more severe trabecular bone damage occurred in the adenine-induced CKD model rats. Based on the results from these previous studies and the present study, although cortical BMD decreased in both 5/6 nephrectomized rats and adenine-induced CKD model rats, the effects of CKD on trabecular bone may differ based on the duration of the condition of CKD, the strain of animals, the time points of evaluation, and a high-phosphorus diet. Further evaluation is needed to evaluate the effects on trabecular bone in adenine-induced CKD model Wistar rats.

4.4. Changes of cortical BMD, bone strength, and micro-architecture

CKD causes bone loss, particularly in cortical bone, through formation of cortical porosities, which lead to skeletal fragility [29]. This has been considered to be caused by the increased PTH level, which is secondary hyperparathyroidism [32,33]. Metzger et al. [30] reported that cortical porosity was reduced after suppression of the PTH level by calcium supplementation. Although the increased PTH did not cause cortical porosity at the distal metaphysis in the adenine-induced CKD model rats in the present study, the parameters of micro-structure of the cortical bone, such as cortical thickness and cortical area, were deteriorated even at the cortical bone of the distal metaphysis. Moreover, the accumulation of uremic toxins, such as indoxyl sulfate and p-cresyl sulfate, could reduce the expression of PTH receptors in osteoblasts and is associated with skeletal resistance to PTH [18]. These skeletal changes including decreased cortical bone area and cortical thickness could cause the decreased bone strength at the distal metaphysis of the femur on the compression test.

4.5. Limitations

The present study demonstrated that adenine-induced CKD model rats had stage IV CKD with deteriorations of trabecular and cortical bone continuing from 12 to 20 weeks. This model of CKD should be appropriate for investigating the effectiveness of treatment for bony changes in future studies. However, there are several limitations in this study. First, the serum estimated glomerular filtration rate was not measured to confirm stage IV CKD in these adenine-induced CKD model rats. Second, there were no evaluations with dynamic bone histomorphometry. Third, changes in parameters of bone quality such as serum pentosidine levels were not examined in this study.

Table 5
Bone strength by the mechanical compression test at the distal metaphysis of the femur.

	Sham (n = 7)			P-value	CKD (n = 7)			P-value
	12 W	16 W	20 W	ANOVA	12 W	16 W	20 W	ANOVA
Stiffness, N/mm	125.8 ± 69.0	270.5 ± 70.9[a]	218.6 ± 137.1	0.011	174.5 ± 41.8	101.8 ± 32.8[a]*	195.4 ± 112.0	0.010
Breaking energy, N.mm	692.8 ± 88.2	682.3 ± 124.6	966.9 ± 117.7[a,b]	< 0.001	306.4 ± 40.5*	580.1 ± 124.4[a]	738.1 ± 167.2[a]*	< 0.001
Maximum load, N	354.2 ± 42.6	339.7 ± 54.4	488.6 ± 66.9[a,b]	< 0.001	144.2 ± 26.1*	357.2 ± 74.9[a]	400.5 ± 70.0[a]*	< 0.001

Values are mean ± standard deviation.
a: P < 0.05 vs 12 W, b: P < 0.05 vs 16 W in the sham or CKD group by post hoc test.
*: P < 0.05 vs sham at the same weeks by unpaired *t*-test.

5. Conclusions

The present study demonstrated that the CKD model rats induced by 0.75% adenine treatment for 4 weeks developed stage IV CKD at 20 weeks. The serum I-PTH level and the percentage of renal fibrosis were higher in the CKD model rats during the experimental period, reflecting the advanced CKD and secondary hyperparathyroidism. Whole-body BMD, micro-architecture of cortical bone, and cortical, as well as trabecular, bone strength were decreased in the CKD model rats. These CKD model rats should be appropriate to evaluate the effects of several treatments for CKD-related osteoporosis and MBD.

CRediT author statement

Hikaru Saito: Investigation, Validation, Visualization, Writing – original draft. **Naohisa Miyakoshi:** Conceptualization, Methodology, Project administration, Writing – review & editing. **Yuji Kasukawa:** Conceptualization, Methodology, Writing – review & editing. **Koji Nozaka:** Investigation, Formal analysis. **Hiroyuki Tsuchie:** Investigation, Formal analysis. **Chiaki Sato:** Investigation. **Kazunobu Abe:** Investigation. **Ryo Shoji:** Investigation. **Yoichi Shimada:** Conceptualization, Funding acquisition, Supervision.

Conflicts of interest

The authors declare no competing interests.

Acknowledgments

The authors would like to thank Ms. Kudo for her support of our experiments. **ORCID** Hikaru Saito: 0000-0002-8901-3232. Naohisa Miyakoshi: 0000-0001-5175-3350. Yuji Kasukawa: 0000-0001-7008-675X. Koji Nozaka: 0000-0003-0238-8929. Hiroyuki Tsuchie: 0000-0001-5011-7184. Chiaki Sato: 0000-0002-3728-8154. Kazunobu Abe: 0000-0002-4991-4239. Ryo Shoji: 0000-0003-1255-6308. Yoichi Shimada: 0000-0002-6523-3249.

References

[1] Levey AS, Atkins R, Coresh J, Cohen EP, Collins AJ, Eckardt KU, et al. Chronic kidney disease as a global public health problem: approaches and initiatives - a position statement from Kidney Disease Improving Global Outcomes. Kidney Int 2007;72:247–59.
[2] Pazianas M, Miller PD. Osteoporosis and chronic kidney disease-mineral and bone disorder (CKD-MBD): back to basics. Am J Kidney Dis 2021;78:582–9.
[3] Nickolas TL, McMahon DJ, Shane E. Relationship between moderate to severe kidney disease and hip fracture in the United States. J Am Soc Nephrol 2006;17:3223–32.
[4] Yenchek RH, Ix JH, Shlipak MG, Bauer DC, Rianon NJ, Kritchevsky SB, et al. Bone mineral density and fracture risk in older individuals with CKD. Clin J Am Soc Nephrol 2012;7:1130–6.
[5] West SL, Lok CE, Langsetmo L, Cheung AM, Szabo E, Pearce D, et al. Bone mineral density predicts fractures in chronic kidney disease. J Bone Miner Res 2015;30:913–9.
[6] Nickolas TL, Stein EM, Dworakowski E, Nishiyama KK, Komandah-Kosseh M, Zhang CA, et al. Rapid cortical bone loss in patients with chronic kidney disease. J Bone Miner Res 2013;28:1811–20.
[7] Metzger CE, Swallow EA, Stacy AJ, Allen MR. Strain-specific alterations in the skeletal response to adenine-induced chronic kidney disease are associated with differences in parathyroid hormone levels. Bone 2021;148:115963.
[8] Newman CL, Moe SM, Chen NX, Hammond MA, Wallace JM, Nyman JS, et al. Cortical bone mechanical properties are altered in an animal model of progressive chronic kidney disease. PLoS One 2014;9:e99262.
[9] Alem AM, Sherrard DJ, Gillen DL, Weiss NS, Beresford SA, Heckbert SR, et al. Increased risk of hip fracture among patients with end-stage renal disease. Kidney Int 2000;58:396–9.
[10] Ensrud KE, Lui LY, Taylor BC, Ishani A, Shlipak MG, Stone KL, et al. Renal function and risk of hip and vertebral fractures in older women. Arch Intern Med 2007;167:133–9.
[11] Naylor KL, McArthur E, Leslie WD, Fraser LA, Jamal SA, Cadarette SM, et al. The three-year incidence of fracture in chronic kidney disease. Kidney Int 2014;86:810–8.
[12] Yokozawa T, Zheng PD, Oura H, Koizumi F. Animal model of adenine-induced chronic renal failure in rats. Nephron 1986;44:230–4.
[13] Brulé D, Sarwar G, Savoie L, Campbell J, Van Zeggelaar M. Differences in uricogenic effects of dietary purine bases, nucleosides and nucleotides in rats. J Nutr 1988;118:780–6.
[14] Chung AW, Yang HH, Kim JM, Sigrist MK, Brin G, Chum E, et al. Arterial stiffness and functional properties in chronic kidney disease patients on different dialysis modalities: an exploratory study. Nephrol Dial Transplant 2010;25:4031–41.
[15] Isakova T, Wahl P, Vargas GS, Gutiérrez OM, Scialla J, Xie H, et al. Fibroblast growth factor 23 is elevated before parathyroid hormone and phosphate in chronic kidney disease. Kidney Int 2011;79:1370–8.
[16] Diniz H, Frazão JM. The role of fibroblast growth factor 23 in chronic kidney disease-mineral and bone disorder. Nefrologia 2013;33:835–44.
[17] Kinoshita H, Miyakoshi N, Kasukawa Y, Sakai S, Shiraishi A, Segawa T, et al. Effects of eldecalcitol on bone and skeletal muscles in glucocorticoid-treated rats. J Bone Miner Metabol 2016;34:171–8.
[18] Yamamoto S, Fukagawa M. Uremic toxicity and bone in CKD. J Nephrol 2017;30:623–7.
[19] Miyakoshi N, Fujii M, Kasukawa Y, Shimada Y. Impact of vitamin C on teriparatide treatment in the improvement of bone mineral density, strength, and quality in vitamin C-deficient rats. J Bone Miner Metabol 2019;37:411–8.
[20] Sato C, Miyakoshi N, Kasukawa Y, Nozaka K, Tsuchie H, Nagahata I, et al. Teriparatide and exercise improve bone, skeletal muscle, and fat parameters in ovariectomized and tail-suspended rats. J Bone Miner Metabol 2021;39:385–95.
[21] Kasukawa Y, Miyakoshi N, Itoi E, Tsuchida T, Tamura Y, Kudo T, et al. Effects of h-PTH on cancellous bone mass, connectivity, and bone strength in ovariectomized rats with and without sciatic-neurectomy. J Orthop Res 2004;22:457–64.
[22] Ono Y, Miyakoshi N, Kasukawa Y, Imai Y, Nagasawa H, Tsuchie H, et al. Micro-CT imaging analysis for the effects of ibandronate and eldecalcitol on secondary osteoporosis and arthritis in adjuvant-induced arthritis rats. Biomed Res 2019;40:197–205.
[23] Kanda Y. Investigation of the freely available easy-to-use software 'EZR' for medical statistics. Bone Marrow Transplant 2013;48:452–8.
[24] Malluche HH, Monier-Faugere MC, Blomquist G, Davenport DL. Two-year cortical and trabecular bone loss in CKD-5D: biochemical and clinical predictors. Osteoporos Int 2018;29:125–34.
[25] Iwasaki Y, Kazama JJ, Yamato H, Fukagawa M. Changes in chemical composition of cortical bone associated with bone fragility in rat model with chronic kidney disease. Bone 2011;48:1260–7.
[26] Ota M, Takahata M, Shimizu T, Kanehira Y, Kimura-Suda H, Kameda Y, et al. Efficacy and safety of osteoporosis medications in a rat model of late-stage chronic kidney disease accompanied by secondary hyperparathyroidism and hyperphosphatemia. Osteoporos Int 2017;28:1481–90.
[27] Bajwa NM, Sanchez CP, Lindsey RC, Watt H, Mohan S. Cortical and trabecular bone are equally affected in rats with renal failure and secondary hyperparathyroidism. BMC Nephrol 2018;19:24.
[28] Ni LH, Tang RN, Lv LL, Wu M, Wang B, Wang FM, et al. A rat model of SHPT with bone abnormalities in CKD induced by adenine and a high phosphorus diet. Biochem Biophys Res Commun 2018;498:654–9.
[29] Metzger CE, Swallow EA, Stacy AJ, Allen MR. Adenine-induced chronic kidney disease induces a similar skeletal phenotype in male and female C57BL/6 mice with more severe deficits in cortical bone properties of male mice. PLoS One 2021;16:e0250438.
[30] Metzger CE, Swallow EA, Stacy AJ, Allen MR. Strain-specific alterations in the skeletal response to adenine-induced chronic kidney disease are associated with differences in parathyroid hormone levels. Bone 2021;148:115963.
[31] Ferrari GO, Ferreira JC, Cavallari RT, Neves KR, dos Reis LM, Dominguez WV, et al. Mineral bone disorder in chronic kidney disease: head-to-head comparison of the 5/6 nephrectomy and adenine models. BMC Nephrol 2014;15:69.
[32] Tamagaki K, Yuan Q, Ohkawa H, Imazeki I, Moriguchi Y, Imai N, et al. Severe hyperparathyroidism with bone abnormalities and metastatic calcification in rats with adenine-induced uraemia. Nephrol Dial Transplant 2006;21:651–9.
[33] Katsumata K, Kusano K, Hirata M, Tsunemi K, Nagano N, Burke SK, et al. Sevelamer hydrochloride prevents ectopic calcification and renal osteodystrophy in chronic renal failure rats. Kidney Int 2003;64:441–50.